An untrasensitive hot-electron bolometer for low-background SMM applications

David Olaya[a,*] , Jian Wei[a,*] , Sergei Pereverzev[a], Boris S. Karasik[b], Jonathan H. Kawamura[b], William R. McGrath[b], Andrei V. Sergeev[c], and Michael E. Gershenson[a]
[a] Department of Physics and Astronomy, Rutgers University, 136 Frelinghuysen Rd., Piscataway, NJ 08854, USA
[b] Jet Propulsion Laboratory, California Institute of Technology, Pasadena, CA 91109, USA
[c] SUNY at Buffalo, Buffalo, NY 14260, USA

ABSTRACT

We are developing a hot-electron superconducting transition-edge sensor (TES) that is capable of counting THz photons and operates at $T = 0.3$K. The main driver for this work is moderate resolution spectroscopy ($R \sim 1000$) on the future space telescopes with cryogenically cooled (~ 4 K) mirrors. The detectors for these telescopes must be background-limited with a noise equivalent power (*NEP*) ~ 10^{-19}-10^{-20} W/Hz$^{1/2}$ over the range $\nu = 0.3$-10 THz. Above about 1 THz, the background photon arrival rate is expected to be ~ 10-100 s^{-1}, and photon counting detectors may be preferable to an integrating type. We fabricated superconducting Ti nanosensors with a volume of ~ 3×10^{-3} μm^3 on planar Si substrate and have measured the thermal conductance G to the thermal bath. A very low $G = 4\times10^{-14}$ W/K, measured at 0.3 K, is due to the weak electron-phonon coupling in the material and the thermal isolation provided by superconducting Nb contacts. This low G corresponds to *NEP*(0.3K) = 3×10^{-19} W/Hz$^{1/2}$. This Hot-Electron Direct Detector (HEDD) is expected to have a sufficient energy resolution for detecting individual photons with $\nu > 0.3$ THz at 0.3 K. With the sensor time constant of a few microseconds, the dynamic range is ~ 50 dB.

Keywords: radiation detectors, submillimeter wave detectors, bolometers, superconducting devices.

1. INTRODUCTION

Several advanced space submillimeter astronomy missions (Single-Aperture FIR Observatory – SAFIR [1,2], Submillimeter Probe of the Evolution of Cosmic Structure – SPECS [3], Space Infrared Telescope for Cosmology and Astrophysics – SPICA [4]) have been recently proposed. These missions will make a dramatic impact on the achievable sensitivity in the spectrometer with moderate resolution ($R = \nu/\Delta\nu \sim 1000$) due to active cooling of telescope mirrors down to ~ 4 K. This deep cooling would significantly reduce the telescope emissivity and enable realization of the background-limited noise equivalent power (*NEP*) ~ 10^{-19}-10^{-20} W/Hz$^{1/2}$ at submillimeter wavelengths (see Fig. 1). However, the *NEP* of state-of-the-art direct detectors [2,5] needs to be lowered by almost two orders of magnitude to meet this goal. Several concepts aimed at the improvement of the sensitivity of THz detectors have been proposed and studied. They include superconducting [6] or normal-metal [7] hot-electron bolometers, kinetic inductance detectors [8,9], membrane-isolated transition-edge bolometers [10], superconducting tunnel-junction devices with single-electron transistor readout [11], hot-spot superconducting detectors [12], and quantum-dot devices [13]. The membrane supported bolometers have come close to meeting the sensitivity goals [10]: a low phonon conductance has been achieved in long (~ 8 mm) Si_3N_4 beams suggesting an *NEP* ~ 10^{-19} W/Hz$^{1/2}$ in the 50-100 mK temperature range. The further decrease of the thermal conductance is hindered by the weakening of the temperature dependence of the thermal conductance due to transition to ballistic phonon transport.

[*] These authors contributed equally to this work.

Besides the more traditional photon-integrating mode of operation, a photon counting mode may be required to achieve the lowest *NEP*. Figure 1 shows that background-limited operation above 1 THz would correspond to a very low photon arrival rate:

$$N_{ph} = \frac{1}{2}\left(\eta \frac{NEP}{h\nu}\right)^2 < 100 \text{ s}^{-1}, \quad (1)$$

(η is the optical coupling efficiency). A detector with a time constant τ will integrate a photon flux if $N_{ph}\tau >> 1$. Therefore, a background limited integrating detector must have a time constant of 0.1 s or greater. Such a long time constant is problematic for many detector concepts: typically, τ does not exceed a few milliseconds for hot-electron detectors and kinetic inductance detectors, so they both would have to operate in the photon counting mode for the detection of weak signals. Although the photon counting mode in the THz range has been considered in several papers (see, e.g., [11,12,14]), the detection of individual THz photons has been demonstrated only using the quantum-dot devices [13]. The latter approach has been recently advanced towards practical application in terahertz microscopy [15] but there is still a long way to go towards the development of an array of such detectors for space instruments.

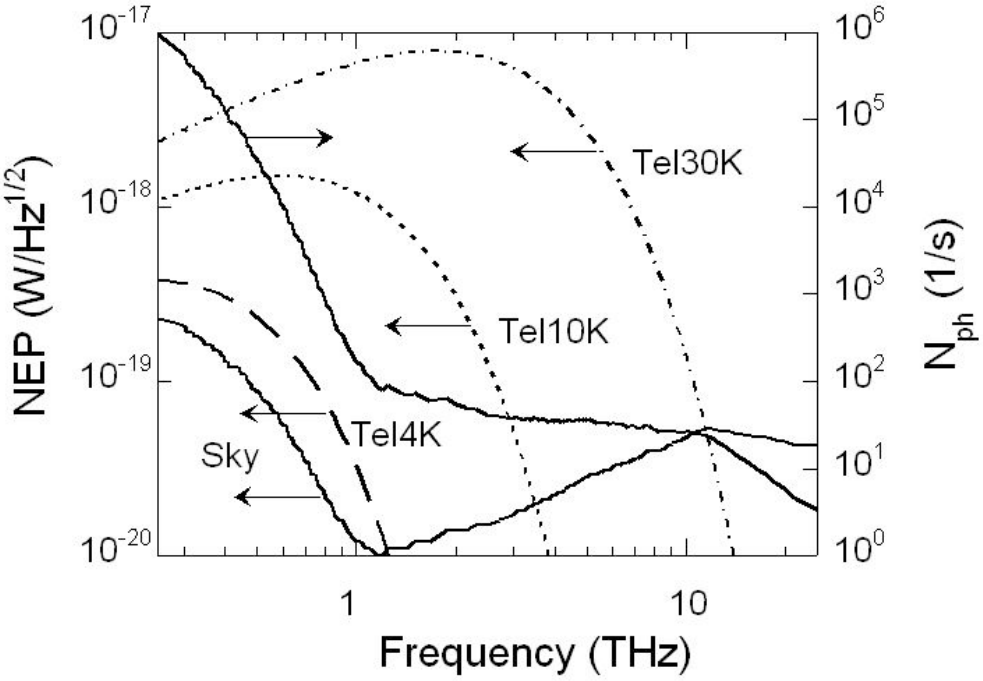

Fig. 1. The *NEP* limited by the background and by the telescope emission (5% emissivity, mirror temperature 4K, 10K, and 30K) for a moderate resolution spectrometer ($\nu/\Delta\nu$ = 1000, single mode) and the arrival rate for background photons. The latter is less than 100 s^{-1} above 1 THz. Below 1 THz, the major contribution is due to the Cosmic Microwave Background radiation; at higher frequencies, radiation from the galactic core and dust clouds dominates.

2. HOT-ELECTRON DIRECT DETECTOR

We are pursuing a Hot-Electron Direct Detector (= hot-electron TES), which can operate in both photon-integrating and photon-counting modes at 0.3 K. The idea of improving the sensitivity of bolometers by employing the hot-electron effects at ultra-low temperatures has been developed by several groups over a number of years [6,7,16,17,18]. The fundamental limit of the *NEP* is set in this case by the thermal energy fluctuations:

$$NEP = \sqrt{2k_B T_e^2 \, C_e(T_e,V)/\tau_{e-ph}(T_e)} \ . \qquad (2)$$

Here $C_e = \gamma V T_e$ is the electron heat capacity, V is the sensor volume, γ is the Sommerfeld constant, and $\tau_{e\text{-}ph}$ is the electron-phonon energy relaxation time. The sensitivity increases with decreasing the sensor volume and lowering the electron temperature T_e. Especially strong is the effect of lowering T_e: $NEP_{\text{e-ph}} \sim T_e^{7/2}$ because of a very rapid increase of the electron-phonon relaxation time $\tau_{\text{e-ph}} \propto T_e^{-4}$ in disordered conductors at ultra-low temperatures (see, e.g., [19,20]). Since the electron temperature is always $\sim T_C$ in hot-electron TES, then lowering T_e requires reducing T_C to the desired level. This can be achieved by magnetic ion implantation, e.g. $^{+}Mn^{55}$ ions work well on Ti [21]. Using conventional nanolithographic methods, the volume of metallic nanostructures can be reduced down to $\sim 10^{-21}$ m^3, which translates into $C_e(0.3\text{ K}) \sim 10^{-19}$ J/K. For such a nanosensor, the predicted *NEP* can be 10^{-19} W/Hz$^{1/2}$ at $T \approx 0.3$ K and 10^{-20} W/Hz$^{1/2}$ at $T \approx 0.1$ K [6]. However, even a record long $\tau_{e\text{-}ph} \sim 20$ ms measured in thin Hf and Ti films at 40 mK [20] is insufficiently long for integrating photons with $N_{ph} \sim 100$ s^{-1}.

Equation (2) assumes that the electron-phonon relaxation is the only mechanism of energy dissipation. To prevent the energy flow from the antenna-coupled nanosensor, the electrical leads to the nanostructure should be made of a superconductor with a sufficiently large superconducting gap: in this case, while electrical current can freely flow across the normal metal-superconductor interface, the outdiffusion of "hot" electrons is blocked by Andreev reflection [22,7]. The detector design should also ensure the suppression of photon emission by electrons in the frequency range corresponding to the operating temperature 0.3K (~ 10 GHz) [23]; this, however, can be achieved simultaneously with a good impedance match between the sensor and the embedded circuit.

We have been systematically working on the realization of ultra-sensitive HEDDs for a number of years [6,20,24,25] and recently achieved the expected thermal characteristics in nanoscale Ti HEDDs with Nb Andreev contacts.

2.1. Device fabrication and thermal conductance measurements

The device fabrication routine was similar to that described in our earlier paper [25]. The HEDD element is a transition edge nanosensor made from thin Ti film with superconducting transition temperature $T_C \sim 0.2\text{-}0.4$ K. The current leads to the nanosensor are fabricated from Nb films with $T_C \sim 8.5$ K; a large superconducting gap in Nb blocks outdiffusion of "hot" electrons to the current leads. The nanostructure is fabricated on a silicon substrate using electron-beam lithography and e-gun deposition of Ti and Nb. For the fabrication of an oxide-free Ti/Nb interface, we have used the well-known "shadow mask" technique: Ti and Nb films were sequentially deposited at different angles through a "shadow" mask without breaking vacuum. The mask was designed in a way to make sure that Nb film covers only the ends of the Ti nanosensor.

A typical Ti device is shown in Fig. 2. Among different tested devices the normal-state resistance ranges between 50-100 Ohm and the critical temperature is between 0.2-0.4 K. The minimum device width is set by the e-beam lithography. Further reduction of the device length is problematic [6]: for nanosensors with length comparable to the thermal length $L_C = \sqrt{\hbar D / k_B T}$, where D is the diffusion constant, the superconducting transition temperature will be significantly increased due to the proximity effect between Ti nanosensor and Nb current leads. For the studied Ti films with diffusion constant $D \sim 4$ cm^2/s, L_C is of the order of 0.1 μm at $T = 0.3$K. Also, if the length of the Ti nanosensor is smaller than the electron thermalization length, the frequency-dependent response and drop in sensitivity might be expected at $h\nu > \Delta_{\text{Nb}}$ ($\nu > 0.3$ THz). For this reason we do not make HEDD devices shorter than ~ 0.5 μm.

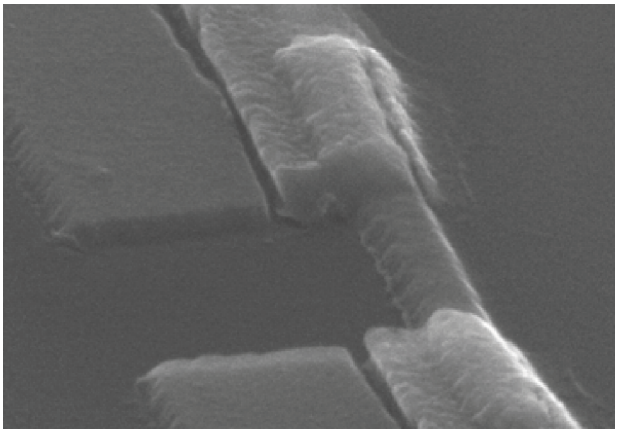

Fig. 2. SEM image of a Ti nanosensor. The Ti nanosensor with dimensions 0.04μm × 0.14μm × 0.56μm is flanked by Nb current leads (Ti is dark gray and Nb is light gray). The rest of Ti film is separated from the Ti nanosensor and Nb leads by trenches.

Measurements of the thermal conductance G have been performed in the dilution refrigerator equipped with several stages of low-pass electical filters thermally anchored to the 1K pot and mixing chamber; the filters were designed to suppress both the low-frequency interferences and rf noise over the frequency range from kHz to several GHz. Because of high sensitivity, the devices can be overheated above their superconducting transition temperature by electromagnetic noise with the power $\delta T_C C_e/\tau_{e\text{-}ph} \leq 1$ fW.

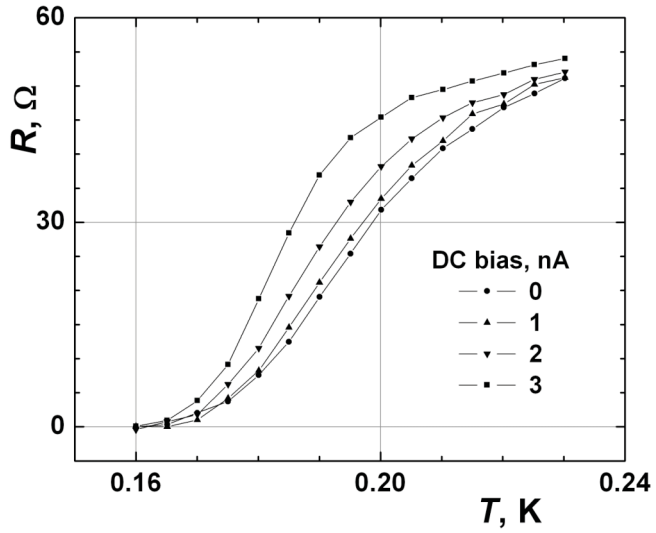

Fig. 3. Measurements of the thermal conductivity between the electrons in a Ti HEDD device with dimensions 0.04μm × 0.14μm × 0.56μm and the thermal bath. The shift of the superconducting transition is caused by the Joule heat generated in the sample by the DC bias current.

Figure 3 illustrates the measurement of the thermal conductance $G = C_e/\tau_{e\text{-}ph}$ between the electrons in a nanosensor and the thermal bath. The resistance of devices was measured by an AC (13 Hz) resistance bridge using a small (typically, 0.1-1 nA) measuring current. The Ti nanosensor was slightly heated by a DC current, and the difference between the electron temperature T_e and the equilibrium bath temperature T_{ph} was determined by observing the temperature shift of the superconducting transition. This method assumes that the non-equilibrium electron distribution function can be characterized with an effective electron temperature. This assumption is valid at sub-Kelvin temperatures, where the electron-electron scattering rate in thin films exceeds by many orders of magnitude the electron-phonon scattering rate

[16]. To measure G at $T < T_C$ the superconducting transition was suppressed to lower temperatures by applying a magnetic field perpendicular to the plane of the nanosensor. The thermal conductivity was found from the balance equation:

$$RI_{DC}^2 = G(T_e)(T_e - T_{ph}), \quad (3)$$

which holds if $T_e - T_{ph} << T_{ph}$. For the device with dimensions 0.04μm × 0.14μm × 0.56μm (Fig. 2), we obtained $G(0.3\text{K}) = 4\times10^{-14}$ W/K. The value of G normalized to volume $G(0.3\text{K})/V = 1.2\times10^{7}$ W/(K·m^3) agrees very well with the corresponding value of G/V measured for much larger meander-patterned Ti films with dimensions 0.04μm × 5μm × 100,000μm (note that the length of 10 cm for the latter structures is much greater than the diffusion length over the electron-phonon relaxation time, $L_{e-ph} = (D\tau_{e-ph})^{1/2}$). The scaling of G with the sensor volume (over 6 orders of magnitude) provides an experimental proof that in both types of structures, the nanostructures with superconducting contacts and much larger Ti meanders, the dominant mechanism of energy dissipation at $T = 0.3$K is electron-phonon scattering, and that the energy relaxation due to outdiffusion of hot electrons can be neglected. The measured values of G are in good agreement with the estimate of G on the basis of the theory of electron-phonon energy relaxation in disordered conductors [19] and our previous measurements of the electron-phonon relaxation rate in disordered Ti films [20].

2.2. Modeling of the device performance

The Ti HEDD will operate in the voltage-biased TES mode; that is, its operating temperature will be somewhat lower than T_C, and the resistance at the operating point, R, will be much smaller than the normal resistance R_N. This biasing mode enables the device to simultaneously match to the antenna impedance and couple well to the SQUID. Indeed, if the DC resistance at the operating point is ~ 1 Ω, the device Johnson noise would exceed the noise of a typical DC SQUID; at the same time, a much higher impedance of the device in the THz range (~ 50-100 Ω) facilitates coupling of the device to a planar antenna. The signal photon will be absorbed and increase the electron temperature in the nanosensor. The increase in electron temperature will cause the current to decrease, and will be registered by the SQUID-based readout. The response time of these devices is controlled by the electron-phonon energy relaxation time τ_{e-ph} (~5-20 μs at 0.3K, depending on disorder in Ti films and substrate material.). If necessary, the response time can be further reduced by using the negative electrothermal feedback (ETF) [26]: $\tau = \tau_{e-ph}/(1+L)$, where L is the ETF loop gain.

In the photon integrating mode, the thermal-fluctuations-limited *NEP* for the developed HEDD with dimensions 0.04μm × 0.1μm × 0.5μm will be less than 3×10^{-19} W/Hz$^{1/2}$ at 0.3 K (see Eq. 2). Since the time constant of the detector is not sufficiently long to integrate the background photons arriving at a rate < 100 s^{-1}, the photon-counting mode should be used to achieve the highest sensitivity at $\nu > 1$ THz. The energy resolution in this mode is limited by the thermal energy fluctuations and the Johnson noise [26]:

$$\delta E = \left(4\sqrt{n/2}\, k_B T_e^2 C_e / \alpha\right)^{1/2}. \quad (4)$$

Here $\alpha = \partial \ln R / \partial \ln T$ ($= 2T_C/\delta T_C \approx 60$ for our samples), $n = 5$-6 is the exponent in the electron-phonon thermal conductance ($G_{e-ph} \sim T^n$). For the device with dimensions 0.04μm × 0.1μm × 0.5μm, the estimated energy resolution, δE, corresponds to the "red boundary" $\nu_R = \delta E/h = 0.24$ THz. The value of $N_{max} \approx \tau^{-1}$ [14] determines the maximum count rate; this value can be as large as ~ 1×10^{6} s^{-1} at $T = 0.3$K. This would provide a large dynamic range for the counter: $N_{max}/N_{ph}^{1/2} \sim 50$ dB ($N_{ph}^{1/2}$ is the minimum signal which can be distinguished from the background).

In order to achieve the background-limited performance, the dark count rate in the device, N_d, must be lower than N_{ph}. The fundamental dark counts are caused by spikes in the device phonon noise that can be mistaken for the signal. To avoid this, an appropriate level of the discrimination threshold, $E_T < h\nu$, must be chosen for the photon counter. However, setting E_T too high may reduce the intrinsic quantum efficiency of the detector: the photon remains undetected if the sum of a negative noise spike and a positive signal caused by an absorbed photon is lower than the threshold. The analysis based on Poisson statistics [14] shows that for $\nu = 1$ THz setting $E_T \approx 3.5\delta E$ provides both quantum efficiency ≈ 100% and $NEP < 10^{-20}$ W/Hz$^{1/2}$.

3. CONCLUSION

We have demonstrated a superconducting Hot-Electron Direct Detector with a record-low *NEP* = 3×10^{-19} W/Hz$^{1/2}$ at 0.3 K. This operating temperature can be achieved by He3 sorption cooling; for comparison, similar sensitivity in the conventional bolometers can be realized only at 0.1K or below, which requires dilution refrigeration or adiabatic demagnetization cooling techniques. In its most sensitive photon counting mode, this detector would be suitable for a background limited spectrometer with moderate resolution (R~1000) for SAFIR and other space-born far-IR telescopes with cryogenically cooled mirrors. For higher background applications (e.g., CMBPol), HEDD offers the background limited sensitivity at T = 0.3K. The hot-electron detectors have two other important advantages: (a) they are fabricated on bulk substrates, and (b) they have a very short time constant allowing for a high data rate. The HEDDs can be readily matched to a planar antenna since the device RF impedance is in the range 50-100 Ω and the device size is much smaller than the wavelength. As with other transition-edge sensors, the HEDD is compatible with SQUID-based multiplexing read-out circuits.

4. ACKNOWLEDGMENTS

The work at Rutgers was supported in part by the NASA grant NNG04GD55G and by the Rutgers Academic Excellence Fund. The research of BSK, WRM and JHK was carried out at the Jet Propulsion Laboratory, California Institute of Technology, under a contact with the National Aeronautics and Space Administration.

REFERENCES

1. http://safir.jpl.nasa.gov/technologies.shtml.
2. D.J. Benford and S.H. Moseley, “Cryogenic detectors for infrared astronomy: the Single Aperture Far-InfraRed (SAFIR) Observatory,” *Nucl. Instr. Meth. Phys. Res. A* 520(1-3), 379-383 (2004).
3. D. Leisawitz, “NASA's far-IR/submillimeter roadmap missions: SAFIR and SPECS,” *Adv. Space Res.* 34(3), 631-636 (2004).
4. T. Nakagawa, “SPICA: space infrared telescope for cosmology and astrophysics,” *Adv. Space Res.* 34(3), 645-650 (2004).
5. J.J. Bock, P. Day, A. Goldin, H.G. LeDuc, C. Hunt, A. Lange et al., “Antenna-coupled bolometer array for astrophysics,” *Proc. Far-IR, SubMM & MM Detector Technology Workshop, April 1-3, 2002, Monterey, CA*, 224-229.
6. B.S. Karasik, W.R. McGrath, H.G. LeDuc, and M.E. Gershenson, “A hot-electron direct detector for radioastronomy,” *Supercond. Sci. Technol.* 12(11), 745-747 (1999); B.S. Karasik, W.R. McGrath, M.E. Gershenson, and A.V. Sergeev, “Photon-noise-limited direct detector based on disorder-controlled electron heating,” *J. Appl. Phys.* 87(10), 7586-7588 (2000).
7. M.Nahum and J.M. Martinis, "Ultrasensitive hot-electron microbolometer," *Appl. Phys. Lett.* 63, 3075-3077 (1993); A. Vystavkin, D. Chouvaev, L. Kuzmin, M. Tarasov, E. Aderstedt, M. Willander, and T. Claeson, “Andreev reflection based normal metal hot-electron bolometer for space applications,” *Proc. SPIE* 3465, 441-448 (1998).
8. A.V. Sergeev, V.V. Mitin, and B.S. Karasik, “Ultrasensitive hot-electron kinetic-inductance detectors operating well below superconducting transition,” *Appl. Phys. Lett.* 80(5), 817-819 (2002).
9. P.K. Day, H.G. LeDuc, B.A. Mazin, A. Vayonakis, and J. Zmuidzinas, “A broadband superconducting detector suitable for use in large arrays,” *Nature* 425, 817-821 (2003).
10. M. Kenyon, P.K. Day, C.M. Bradford, J.J.Bock, and H.G. Leduc, "Background-imited membrane-isolated TES bolometers for far-IR/submillimeter direct-detection spectroscopy," *Nucl. Instr. & Meth. Phys. Res. A* 559, 456-458 (2006).
11. R.J. Schoelkopf S.H. Moseley, C.M. Stahle, P. Wahlgren, and P. Delsing, “A concept for a submillimeter-wave single-photon counter,” *IEEE Trans. Appl. Supercond.* 9(2), Pt.3, 2935-2939 (1999).
12. A. Semenov, A. Engel, K. Il’in, G. Gol'tsman, M. Siegel and H.W. Hubers, “Ultimate performance of a superconducting quantum detector,” *Eur. Phys. J. Appl. Phys.* 21(3), 171-178 (2003).
13. S. Komiyama, O. Astafiev, V. Antonov, T. Kutsuwa, and H. Hirai, ”A single-photon detector in the far-infrared range,” *Nature* 403, 405-407 (2000); O. Astafiev, S. Komiyama, T. Kutsuwa, V. Antonov, Y. Kawaguchi, and

K. Hirakawa, “Single-photon detector in the microwave range,” *Appl. Phys. Lett*. 80(22), 4250-4252 (2002); H. Hashiba, V. Antonov, L. Kulik, S. Komiyama, and C. Stanley, "Highly sensitive detector for submillimeter wavelength range," *Appl. Phys. Lett.* 85(24), 6036-6038 (2004).
14. B.S. Karasik and A.V. Sergeev, “THz Hot-Electron Photon Counter,” *IEEE Trans. Appl. Supercond*. 15(2), 618-621 (2005).
15. K. Ikushima, Y. Yoshimura, T. Hasegawa, S. Komiyama, T. Ueda, and K. Hirakawa, "Photon-counting microscopy of terahertz radiation," *App. Phys. Lett.* 88, 152110 (2006).
16. E. M. Gershenson, M. E. Gershenson, G. N. Goltsman, A. D. Semenov, and A. V. Sergeev, "Heating of electrons in a superconductor in the resistive state by electromagnetic radiation," *Sov.Phys.-JETP* 59, 442-450 (1984).
17. B. Cabrera, R.M. Clarke, P. Colling, A.J. Miller. S. Nam, R.W. Romani, “Detection of single infrared, optical, and ultraviolet photons using superconducting transition edge sensors,” *Appl. Phys. Lett*. 73(6), 735-737 (1998).
18. T.A Lee, P.L. Richards, S.W. Nam, B. Cabrera, and K.D. Irwin, “A superconducting bolometer with strong electrothermal feedback,” *Appl. Phys. Lett.* 69, 1801-1803 (1996).
19. A. Sergeev and V. Mitin, "Electron-phonon interaction in disordered conductors: Static and vibrating scattering potentials," *Phys. Rev. B*. 61(9), 6041-6047 (2000).
20. M.E. Gershenson, D. Gong, T. Sato, B.S. Karasik, A.V. Sergeev, "Millisecond electron-phonon relaxation in ultrathin disordered metal films at millikelvin temperatures," *Appl. Phys. Lett*. 79, 2049-2051 (2001).
21. B.A. Young, J.R. Williams, S.W. Deiker, S.T. Ruggiero, and B. Cabrera, "Using ion implantation to adjust the transition temperature of superconducting films," *Nucl. Inst. Meth. Phys. Res. A* 520, 307-310 (2004).
22. A.F. Andreev, "The thermal conductivity of the intermediate state in superconductors," *Zh. Eksp. Teor. Fiz*. 46, 1823 (1964) [*Sov. Phys. JETP* 19(5), 1228-1231 (1964)].
23. D.R. Schmidt, R.J. Schoelkopf, and A.N. Cleland, “Photon-Mediated Thermal Relaxation of Electrons in Nanostructures,” *Phys. Rev. Lett.* 93, 045901 (2004).
24. B.S. Karasik, B. Delaet, W.R. McGrath, J. Wei, M.E. Gershenson, and A.V. Sergeev, "Experimental Study of Superconducting Hot-Electron Sensors for Submm Astronomy," *IEEE Trans. Appl. Supercond.* 13(2), 188-191 (2003).
25. B.S. Karasik, A.V. Sergeyev, D. Olaya, J. Wei, M.E. Gershenson, J.H. Kawamura, and W.R. McGrath, "A Photon Counting Hot-Electron Bolometer for Space THz Spectroscopy," *Proc. 16th Int. Symp. Space Terahertz Technol., May 2-4, 2005, Gothenburg, Sweden*, 543-548.
26. K.D. Irwin, “An application of electrothermal feedback for high resolution cryogenic particle detection,” *Appl. Phys. Lett.* 66, 1998-2000 (1995).